

Searching for the heavy custodial fiveplet Higgs in the Georgi-Machacek model at the International Linear Collider

YuFei Zhang, Hao Sun*, Xuan Luo, and WeiNing Zhang

*Institute of Theoretical Physics, School of Physics,
Dalian University of Technology, No.2 Linggong Road,
Dalian, Liaoning, 116024, P.R.China*

Abstract

The Georgi-Machacek (GM) model is one of many Beyond Standard Model scenarios with an extended scalar sector which can group under the custodial $SU(2)_C$ symmetry into a fiveplet, a triplet, and two singlets. The heavy charged custodial fiveplet Higgs H_5^\pm are typical particles in GM model which couple to the electroweak gauge bosons, therefore provide a good testing ground for the detection of the $H^\pm W^\mp Z$ vertex. The neutral custodial fiveplet Higgs H_5^0 in the GM model has the same mass with H_5^\pm and couples to the electroweak gauge bosons W^+W^- and ZZ both. We study the discovery prospects of the exotic scalar bosons H_5^\pm and H_5^0 at the International Linear Collider(ILC) via the vector boson associated production processes, and discuss two different decay modes for both charged and neutral scalars. The discovery potential is discussed. Testing the mass degeneracy of charged and neutral scalar bosons in the GM model is also considered.

Keywords: Georgi-Machacek model, ILC

PACS numbers: 12.60.-i ,12.60.Fr

* Corresponding author: haosun@mail.ustc.edu.cn haosun@dlut.edu.cn

I. INTRODUCTION

The discovery of the Higgs boson at the Large Hadron Collider(LHC)[1][2] is a major step towards the understanding of the electroweak symmetry breaking(EWSB) mechanism and marks a new era in particle physics. But this is of course not the end of the story. Besides some long standing problems such as dark matter and neutrino mass, it seems strange that only one scalar boson appears in the Standard Model(SM) particle list, while both fermions and gauge bosons are of rich variety. The structure of the Higgs sector may be more complicated than the minimal form in the SM. It reminds us that even after the discovery of the Higgs boson we may still do not know all the details of the EWSB.

An extended scalar sector is presented in many Beyond Standard Model(BSM) scenarios, for instance, the two Higgs doublet model[3], the minimal supersymmetric model[4], the left-right symmetric model[5], the little Higgs model[6] and the Georgi-Machacek model [7][8]. The Georgi-Machacek(GM) model is one scenario proposed in the mid 80s extending the SM Higgs sector with a complex $SU(2)_L$ doublet field ϕ ($Y = 1$), a real triplet field ξ ($Y = 0$) and a complex $SU(2)_L$ triplet field χ ($Y = 2$), where Y is the hypercharge. In the GM model, the scalar potential maintains custodial $SU(2)_C$ symmetry which can keep the electroweak ρ parameter at unity at tree level[9] to be consistent with the experimental data. After symmetry breaking, the physical fields can be organized by their transformation properties under the custodial $SU(2)_C$ symmetry into a fiveplet, a triplet, and two singlets. At the tree level the fiveplet scalars couple to the electroweak gauge bosons but not SM fermions, whereas the triplet scalars couple to the fermions but not the gauge bosons. Moreover, the model can naturally provides tiny neutrino mass via the well known Type-II Seesaw Mechanism[10]. There have been extensive phenomenological studies of the exotic Higgs bosons in the GM model in the literature[11–16]. The effect of enhancing the Higgs couplings to weak gauge bosons has also been considered[17–20]. In this work, we investigate the discover potential of the charged and neutral fiveplet scalars in the GM model at the International Linear Collider(ILC).

The charged Higgs bosons appear in many BSM, and the process involving the vertex $H^\pm W^\mp Z$ can be one of the most promising channel to discover the charged Higgs bosons[21]. In Ref.[22], the measurement of this vertex has been discussed using the recoil method at the ILC, where H^\pm is assumed to decay leptonically due to its small mass. In the case of a heavy H^\pm , the decay channel to $W^\pm Z$ is open and the phenomenology would be more complicated and interesting. At the tree level the fiveplet in the GM model couple to the electroweak gauge bosons but not SM

fermions, in particular, the $H_5^\pm W^\mp Z$ vertex appears. In the Higgs extended models with singly charged Higgs bosons, the vertex $H^\pm W^\mp Z$ appears at tree level only when H^\pm comes from an exotic representation such as triplets. It is absent at tree level if H^\pm comes from a doublet. Therefore, this vertex can be used to distinguish models with singly charged Higgs bosons[22]. In this paper, based on the framework of GM model, we perform the signal and background simulation of the process $e^+e^- \rightarrow H_5^\pm W^\mp \rightarrow W^\pm W^\mp Z$ at detector level at the ILC. There are mainly three types of the production modes of H_5^\pm , namely, the pair production of singly-charged bosons, the vector boson associated production, and the vector boson fusion processes. We are interested in the coupling of the $H_5^\pm W^\mp Z$ vertex, therefore the channel we consider is vector boson associated(VBA) production processes. There are two VBA processes, one is $e^+e^- \rightarrow Z \rightarrow H_5^\pm W^\mp$, the other is $e^+e^- \rightarrow H_3^0 \rightarrow H_5^\pm W^\mp$, where H_3^0 is the neutral triplet. The latter process also involves the coupling $g_{eeH_3^0} = -\frac{m_e}{v} \tan\theta_H \gamma_5$, in which $v \approx 246$ GeV is the vacuum expectation value in the SM, $\tan\theta_H = \frac{2\sqrt{2}v_X}{v_\phi}$, and v_X, v_ϕ are the vacuum expectation values (vevs) of the triplet and doublet respectively. Thus this process is highly suppressed due to the smallness of the electron mass compared to the vacuum expectation value in the SM.

One of the most distinguished feature of the GM model is that particles within each multiplet have the same mass at tree level. The particle H_5^0 couples to ZZ and W^+W^- both. Therefore it can be produced in vector boson associated production process at the ILC. We have also studied the phenomenology of H_5^0 production at the ILC. Testing the mass degeneracy of charged and neutral scalar bosons can be a direct evidence of the GM model. This has also been considered in this paper. Typically, our paper is organized as follows: In Section 2 the GM model is described in detail. The constraints on the parameters of the GM model are also presented. In section 3 we study the collider phenomenology of charged fiveplet resonance at the ILC. In section 4 we study the collider phenomenology of neutral fiveplet resonance at the ILC. The discovery prospects of process B (see the following) in the paper is further discussed in section 5. Testing the mass degeneracy of charged and neutral scalar bosons in the GM model is considered in section 6. Finally we make our conclusions in the last section.

II. SETUP THE MODEL FRAMEWORK

A. Description of the Georgi-Machacek model

The scalar sector of the GM model is composed of a complex $SU(2)_L$ doublet field ϕ ($Y = 1$), a real triplet field ξ ($Y = 0$), and a complex $SU(2)_L$ triplet field χ ($Y = 2$) [23]. The scalar content of the theory can be organized in terms of the $SU(2)_L \otimes SU(2)_R$ symmetry. In order to make this symmetry explicit, we write the doublet in the form of a bidoublet Φ and combine the triplets to form a bitriplet X :

$$\Phi = \begin{pmatrix} \phi^{0*} & \phi^+ \\ -\phi^{+*} & \phi^0 \end{pmatrix}, \quad X = \begin{pmatrix} \chi^{0*} & \xi^+ & \chi^{++} \\ -\chi^{+*} & \xi^0 & \chi^+ \\ \chi^{++*} & -\xi^{+*} & \chi^0 \end{pmatrix}. \quad (1)$$

The vacuum expectation values (vevs) are given by $\langle \Phi \rangle = \frac{v_\phi}{\sqrt{2}} I_{2 \times 2}$ and $\langle X \rangle = v_X I_{3 \times 3}$. The vevs of the two triplets must be the same in order to preserve custodial symmetry and ensure $\rho = \frac{m_W^2}{m_Z^2 \cos^2 \theta_W}$ to be unity at tree level. The neutral fields can be decomposed into real and imaginary parts according to

$$\phi^0 \rightarrow \frac{v_\phi}{\sqrt{2}} + \frac{\phi^{0,r} + i\phi^{0,i}}{\sqrt{2}}, \quad \chi^0 \rightarrow v_X + \frac{\chi^{0,r} + i\chi^{0,i}}{\sqrt{2}}, \quad \xi^0 \rightarrow v_X + \xi^0, \quad (2)$$

and we parameterize the vevs for convenience

$$c_H = \cos \theta_H \equiv \frac{v_\phi}{v}, \quad s_H = \sin \theta_H \equiv \frac{2\sqrt{2} v_X}{v}. \quad (3)$$

The scalar kinetic terms

$$\mathcal{L}_{\text{kin}} = |D_\mu^{(\phi)} \phi|^2 + \frac{1}{2} |D_\mu^{(\xi)} \xi|^2 + |D_\mu^{(\chi)} \chi|^2, \quad (4)$$

give the interaction terms between scalars and the EW gauge bosons. Write out explicitly, we have

$$\begin{aligned} \mathcal{L}_{\text{kin}} \supset & (v_\phi + \phi^{0,r})^2 \left(\frac{g^2}{4} W_\mu^+ W^{-,\mu} + \frac{g^2 + g'^2}{8} Z_\mu Z^\mu \right) + (v_X + \xi^0)^2 (g^2 W_\mu^+ W^{-,\mu}) \\ & + (\sqrt{2} v_X + \chi^{0,r})^2 \left(\frac{g^2}{2} W_\mu^+ W^{-,\mu} + \frac{g^2 + g'^2}{2} Z_\mu Z^\mu \right). \end{aligned} \quad (5)$$

Therefore, the gauge boson masses are given by

$$m_W^2 \equiv \frac{g^2}{4} (v_\phi^2 + 8v_X^2), \quad m_Z^2 \equiv \frac{g^2 + g'^2}{4} (v_\phi^2 + 8v_X^2). \quad (6)$$

So the W and Z boson mass conditions give the following constraint

$$v_\phi^2 + 8v_X^2 \equiv v^2 = \frac{1}{\sqrt{2} G_F} \approx (246 \text{ GeV})^2. \quad (7)$$

The most general gauge invariant scalar potential that conserves custodial $SU(2)_C$ symmetry is given by

$$\begin{aligned} V(\Phi, X) = & \frac{\mu_2^2}{2} \text{Tr}(\Phi^\dagger \Phi) + \frac{\mu_3^2}{2} \text{Tr}(X^\dagger X) + \lambda_1 [\text{Tr}(\Phi^\dagger \Phi)]^2 + \lambda_2 \text{Tr}(\Phi^\dagger \Phi) \text{Tr}(X^\dagger X) \\ & + \lambda_3 \text{Tr}(X^\dagger X X^\dagger X) + \lambda_4 [\text{Tr}(X^\dagger X)]^2 - \lambda_5 \text{Tr}(\Phi^\dagger \tau^a \Phi \tau^b) \text{Tr}(X^\dagger t^a X t^b) \\ & - M_1 \text{Tr}(\Phi^\dagger \tau^a \Phi \tau^b) (UXU^\dagger)_{ab} - M_2 \text{Tr}(X^\dagger t^a X t^b) (UXU^\dagger)_{ab}. \end{aligned} \quad (8)$$

Here $\tau^a = \sigma^a/2$ with σ^a being the Pauli matrices are the $SU(2)$ generators for the doublet representation, t^a are the generators for the triplet representation

$$t^1 = \frac{1}{\sqrt{2}} \begin{pmatrix} 0 & 1 & 0 \\ 1 & 0 & 1 \\ 0 & 1 & 0 \end{pmatrix}, \quad t^2 = \frac{1}{\sqrt{2}} \begin{pmatrix} 0 & -i & 0 \\ i & 0 & -i \\ 0 & i & 0 \end{pmatrix}, \quad t^3 = \begin{pmatrix} 1 & 0 & 0 \\ 0 & 0 & 0 \\ 0 & 0 & -1 \end{pmatrix}, \quad (9)$$

and the matrix U , which rotates X into the Cartesian basis, is given by

$$U = \begin{pmatrix} -\frac{1}{\sqrt{2}} & 0 & \frac{1}{\sqrt{2}} \\ -\frac{i}{\sqrt{2}} & 0 & -\frac{i}{\sqrt{2}} \\ 0 & 1 & 0 \end{pmatrix}. \quad (10)$$

In terms of the vevs, the scalar potential can be written as

$$V(v_\phi, v_X) = \frac{\mu_2^2}{2} v_\phi^2 + 3 \frac{\mu_3^2}{2} v_X^2 + \lambda_1 v_\phi^4 + \frac{3}{2} (2\lambda_2 - \lambda_5) v_\phi^2 v_X^2 + 3 (\lambda_3 + 3\lambda_4) v_X^4 - \frac{3}{4} M_1 v_\phi^2 v_X - 6 M_2 v_X^3. \quad (11)$$

Minimizing this potential yields the following constraints:

$$0 = \frac{\partial V}{\partial v_\phi} = v_\phi \left[\mu_2^2 + 4\lambda_1 v_\phi^2 + 3(2\lambda_2 - \lambda_5) v_X^2 - \frac{3}{2} M_1 v_X \right], \quad (12)$$

$$0 = \frac{\partial V}{\partial v_X} = 3\mu_3^2 v_X + 3(2\lambda_2 - \lambda_5) v_\phi^2 v_X + 12(\lambda_3 + 3\lambda_4) v_X^3 - \frac{3}{4} M_1 v_\phi^2 - 18 M_2 v_X^2. \quad (13)$$

After symmetry breaking, the physical fields can be organized by their transformation properties under the custodial $SU(2)_C$ symmetry into a fiveplet, a triplet, and two singlets. Since under $SU(2)_C$ we have the group representations $(\mathbf{2}, \mathbf{2}) \sim \mathbf{1} \oplus \mathbf{3}$, and $(\mathbf{3}, \mathbf{3}) \sim \mathbf{1} \oplus \mathbf{3} \oplus \mathbf{5}$. One of the two triplets represents the Goldstone bosons and was eaten by the EW gauge bosons. So we get ten physical degrees of freedom: two $SU(2)_C$ singlets ($H_1^0, H_1^{0'}$, correspond to the Higgs and the additional scalar resonance), one $SU(2)_C$ triplet (H_3^+, H_3^0, H_3^-) and one $SU(2)_C$ quintuplet ($H_5^{++}, H_5^+, H_5^0, H_5^-, H_5^{--}$).

The physical states in terms of gauge eigenstates are given by[23]

$$\begin{aligned}
H_5^{++} &= \chi^{++} , \\
H_5^+ &= (\chi^+ - \xi^+)/\sqrt{2} , \\
H_5^0 &= (2\xi^0 - \sqrt{2}\chi^{0,r})/\sqrt{6} , \\
H_3^+ &= \cos\theta_H(\chi^+ + \xi^+)/\sqrt{2} - \sin\theta_H\phi^+ , \\
H_3^0 &= \cos\theta_H\chi^{0,i} - \sin\theta_H\phi^{0,i} , \\
H_1^0 &= \phi^{0,r} , \\
H_1^{0'} &= (\sqrt{2}\chi^{0,r} + \xi^0)/\sqrt{3} .
\end{aligned} \tag{14}$$

Within each custodial multiplet, the masses are degenerate at tree level. Using Eqs. (12–13) to eliminate μ_2^2 and μ_3^2 , the mass of the fiveplet and triplet can be computed. The 2×2 mass-squared matrix of the two custodial SU(2) singlets are given by

$$\mathcal{M}^2 = \begin{pmatrix} \mathcal{M}_{11}^2 & \mathcal{M}_{12}^2 \\ \mathcal{M}_{12}^2 & \mathcal{M}_{22}^2 \end{pmatrix} . \tag{15}$$

Diagonalising the mass matrix, we have two mass eigenstates h and H, defined by

$$\begin{aligned}
h &= \cos\alpha H_1^0 - \sin\alpha H_1^{0'} , \\
H &= \sin\alpha H_1^0 + \cos\alpha H_1^{0'} .
\end{aligned} \tag{16}$$

and the explicit mass formulas can be found in Ref.[23].

B. Constraints on the parameter space of the GM model

1. Theoretical constraints

The theoretical constraints on the parameters of the GM model, such as the unitarity of the perturbation theory and stability of the electroweak vacuum, has been considered in [23].

The $2 \rightarrow 2$ scalar scattering matrix element can be expanded in terms of the Legendre polynomials:

$$\mathcal{A} = 16\pi \sum_J (2J+1) a_J P_J(\cos\theta) , \tag{17}$$

where J is the (orbital) angular momentum and $P_J(\cos\theta)$ are the Legendre polynomials. Perturbative unitarity requires that the zeroth partial wave amplitude, a_0 , satisfy $|a_0| \leq 1$ or $|\text{Re } a_0| \leq \frac{1}{2}$.

In the high energy limit, only those diagrams involving the four-point scalar couplings contribute to $2 \rightarrow 2$ scalar scattering processes; All diagrams involving scalar propagators are suppressed by the square of the collision energy. Therefore the dimensionful couplings M_1 , M_2 , μ_2^2 , and μ_3^2 are not constrained directly by perturbative unitarity. Perturbative unitarity provides a set of constraints on the parameters of the scalar potential[23].

$$\sqrt{P_\lambda^2 + 36\lambda_2^2} + |6\lambda_1 + 7\lambda_3 + 11\lambda_4| < 4\pi, \quad (18)$$

$$\sqrt{Q_\lambda^2 + \lambda_5^2} + |2\lambda_1 - \lambda_3 + 2\lambda_4| < 4\pi, \quad (19)$$

$$|2\lambda_3 + \lambda_4| < \pi, \quad (20)$$

$$|\lambda_2 - \lambda_5| < 2\pi, \quad (21)$$

with $P_\lambda \equiv 6\lambda_1 - 7\lambda_3 - 11\lambda_4$, $Q_\lambda \equiv 2\lambda_1 + \lambda_3 - 2\lambda_4$. In addition

$$\lambda_2 \in \left(-\frac{2}{3}\pi, \frac{2}{3}\pi\right), \quad \lambda_5 \in \left(-\frac{8}{3}\pi, \frac{8}{3}\pi\right). \quad (22)$$

Another constraint comes from the stability of electroweak vacuum, i.e., the potential must be bounded from below. This requirement restricts $\lambda_{3,4}$ to satisfy

$$\lambda_3 \in \left(-\frac{1}{2}\pi, \frac{3}{5}\pi\right), \quad \lambda_4 \in \left(-\frac{1}{5}\pi, \frac{1}{2}\pi\right). \quad (23)$$

2. Experimental constraints

Various measurements of SM quantities in experiments provide stringent constraints on the parameters of GM model. These include:

- Modification of the SM-like Higgs couplings[24]. The Higgs coupling in the GM model depends on the triplet VEV v_X and the mixing angle of the two singlets α . The measured signal strengths of the SM-like Higgs in various channels from a combined ATLAS and CMS analysis of the LHC pp collision data at $\sqrt{s} = 7$ and 8 TeV constrain v_X and α in the GM model severely.
- Electroweak precision tests[25]. The presence of additional scalar states, charged under the EW symmetry, generates a non-zero contribution to the oblique parameters S [26] and T . Setting $U = 0$, the experimental values for the oblique parameters S and T are extracted for a reference SM Higgs mass $m_h^{\text{SM}} = 125$ GeV as $S_{\text{exp}} = 0.06 \pm 0.09$ and $T_{\text{exp}} = 0.10 \pm 0.07$ with a correlation coefficient of $\rho_{ST} = +0.91$. The scalar sector is also constrained by the Z-pole observable $R_b = \frac{\Gamma(Z \rightarrow b\bar{b})}{\Gamma(Z \rightarrow \text{hadrons})}$.

- B-physics observables[25]. Extended Higgs sectors are typically constrained by B-physics observables, such as the branching ratio of $b \rightarrow s\gamma$, the branching ratio of $B_s^0 \rightarrow \mu^+\mu^-$, and $B_s^0 - \bar{B}_s^0$ mixing.

Recently, charged Higgs boson has been searched in the vector-boson fusion mode with decay $H^\pm \rightarrow W^\pm Z$ using pp collisions at LHC. The data based on 20.3 fb^{-1} of proton-proton collision at a center-of-mass energy of 8 TeV recorded with the ATLAS detector at the LHC exclude a charged Higgs boson in the mass range $240 \text{ GeV} < m_{H^\pm} < 700 \text{ GeV}$ within the Georgi-Machacek Higgs Triplet Model with parameter $\sin\theta_H = 1$ and 100% branching fraction of $H^\pm \rightarrow W^\pm Z$ [27]. Moreover, the analysis in Ref.[28] suggests that searches for doubly charged Higgs bosons at the 8 TeV LHC constrain v_X to be small for relatively light fiveplet mass. When a larger value of fiveplet Higgs boson mass m_5 is taken, the bound on v_X becomes more relaxed due to smaller production cross sections. The allowed parameter space of GM model in the plane of $\sin\theta_H$ and fiveplet Higgs boson mass m_5 can be read from Fig.1 in Ref.[29]. Those points were generated by the public available package GMCALC[30], in which various theoretical and experimental constraints are taken into account. It is evident from the plot that m_5 spans a wide range while the $\sin\theta_H$ is constrained from the above. The points above the blue curve are excluded by LHC 8TeV data.

III. SEARCHING FOR H_5^\pm

In this section, we study the collider phenomenology of the heavy charged custodial fiveplet Higgs H_5^\pm production at the ILC. There are mainly three types of the production modes, namely, the pair production of singly-charged bosons, the vector boson associated production, and the vector boson fusion processes. We are interested in the coupling of the $H_5^\pm W^\mp Z$ vertex. Therefore the channel we consider is vector boson associated(VBA) production. The relevant coupling is

$$g_{H_5^+ W^- Z} = -\frac{\sqrt{2}e^2 v_X}{c_w s_w^2}, \quad (24)$$

where c_w and s_w are the cosine and sine of the weak mixing angle, respectively. The process involving $g_{H_5^+ W^- H_3^0}$ can be safely neglected since it also depends on the coupling $g_{e\bar{e}H_3^0} = -\frac{m_e}{v}\tan\theta_H\gamma_5$, and the mass of electron is very small compared to v . Once produced, H_5^\pm decays into different final states according to different couplings. The branching ratio into $W^\pm Z$ is almost 100% when the triplet VEV v_X is relatively large and the custodial triplet has a sufficiently large mass so that it does not deplete the $H_5^\pm \rightarrow W^\pm Z$ branching[13]. In our analysis we have set the custodial triplet mass to be greater than fiveplet mass, so that H_5^\pm has almost 100% branching ratio into $W^\pm Z$.

We study the discovery prospects of H_5^\pm via the decay process $H_5^\pm \rightarrow W^\pm Z$, and investigate its dependence on the triplet VEV v_χ .

We show the center-of-mass energy \sqrt{s} dependence of the cross section of process $e^+e^- \rightarrow H_5^\pm W^\mp$, $H_5^\pm \rightarrow W^\pm Z$ in Fig.1, in which we take $\sin\theta_H = 0.2$. The cross section are suppressed for larger H_5^\pm mass. In the following analysis we focus on the case $m_5 = 300$ GeV, and fix the collision energy to be 500 GeV.

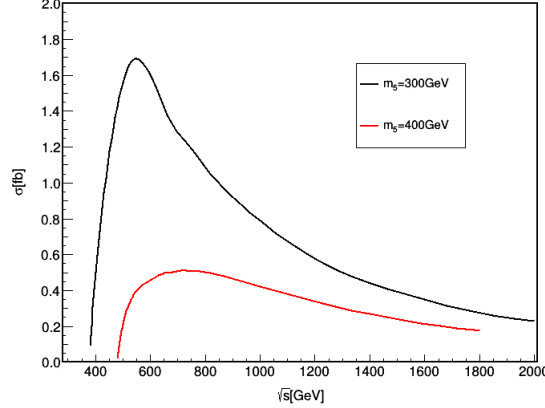


FIG. 1: The cross section of process $e^+e^- \rightarrow H_5^\pm W^\mp$, $H_5^\pm \rightarrow W^\pm Z$ in the GM model as a function of \sqrt{s} .

For the subsequent decay of W^+W^-Z , we consider two cases. In the first case we assume the associated weak gauge boson to decay hadronically, while the $W^\pm Z$ bosons coming from the decay of H_5^\pm decay leptonically, see Fig.2. In this case, we can investigate the possibility of measuring the recoil mass of H_5^\pm by using a recoil method at the ILC[22]. The recoiled mass of H_5^\pm is given in terms of the two jet energy E_{jj} and two jet invariant mass M_{inv}^{jj} as

$$M_{recoil}^2 = s - 2\sqrt{s}E_{jj} + M_{inv}^{jj2}. \quad (25)$$

where s is the center-of-mass energy in the collision. On the other hand, the $3\ell + E_T^{miss}$ system coming from H_5^\pm can be used to construct the transverse mass, which is defined by

$$M_{trans}^2 = [\sqrt{M_{vis}^2 + (\vec{p}_T^{vis})^2} + |E_T^{miss}|]^2 - (\vec{p}_T^{vis} + E_T^{miss})^2 \quad (26)$$

where M_{vis} and \vec{p}_T^{vis} are the invariant mass and the vector sum of the transverse momenta of the charged leptons, respectively, and E_T^{miss} is the missing transverse momentum determined by the negative sum of visible momenta in the transverse direction. The second decay mode we consider is that the associated weak gauge boson decays leptonically, while the Z boson coming from the decay of H_5^\pm decays leptonically and W^\pm coming from H_5^\pm decays hadronically, see Fig.2 for detail. In this case, we can reconstruct the H_5^\pm from the reconstructed W^\pm and Z bosons.

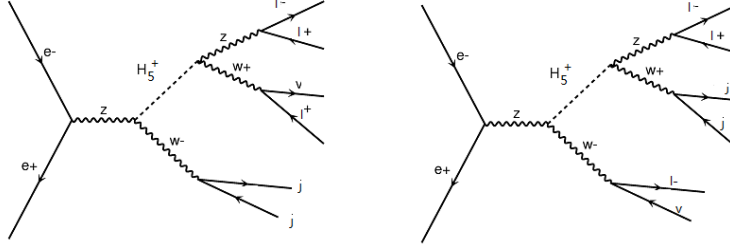


FIG. 2: The Feynman diagrams of the signal process A(left) and B(right) in the GM model.

The main backgrounds for our signal come from the 3- and 4- gauge boson final states in the SM. These include W^+W^-Z , W^+W^-ZZ , $W^+W^-W^+W^-$, ZZZ and $ZZZZ$. For the signal and backgrounds simulation, we use FeynRules[31] to extract the Feynman Rules from the Lagrangian. The model is generated into Universal FeynRules Output(UFO) files[32] and then fed to the Monte Carlo event generator MadGraph@NLO(MG5)[33] for the generation of event samples. Pythia[34] is utilized for showering and hadronisation. We use Delphes[35] to account for the detector simulation. The anti- k_t algorithm[36] with the jet radius of 0.5 is used to reconstruct jets. In all analysis in our paper the initial state radiation is taken into account. We choose bechmark point as follows: The SM inputs are $\alpha_{m_Z} = 1/127.9$, $G_f = 1.16637 \times 10^{-5} \text{ GeV}^{-2}$, $\alpha_s = 0.1184$, $m_Z = 91.1876 \text{ GeV}$, $m_h = 125 \text{ GeV}$. For the GM model inputs we take the fiveplet mass $m_5 = 300 \text{ GeV}$, in this case searches for doubly charged Higgs bosons at the 8 TeV LHC constrain v_X to be smaller than 35 GeV[28], which translates to $\sin\theta_H < 0.4$. We let $\sin\theta_H$ run in the range $[0.1, 0.4]$. In the following we use cut based analysis to optimise the discovery significance which is calculated by the formula:

$$S = \sqrt{2[(n_S + n_B) \log(1 + \frac{n_S}{n_B}) - n_S]} \quad (27)$$

where n_S is the number of signal events and n_B is the number of background events.

A. Process A

In this case the associated weak gauge boson decays hadronically, while the $W^\pm Z$ bosons produced from the decay of H_5^\pm decay leptonically(process A). For event selection we require the final states must contain three leptons, missing transverse energy E_T^{miss} and more than or equal to 2 jets. We reconstruct Z boson by choosing two leptons from final states such that their invariant mass is close to the Z boson mass most and further require that their invariant mass satisfy $m_Z - 20 \text{ GeV} < M_{\text{inv}}^{Z(\ell\ell)} < m_Z + 20 \text{ GeV}$. Similar method is applied to reconstruct W^\pm from jets with the invariant mass of the selected two jets lying in the range $m_W - 20 \text{ GeV} < M_{\text{inv}}^{W(jj)} < m_W + 20 \text{ GeV}$.

The selected events must satisfy the following basic cuts:

$$\begin{aligned}
p_T^\ell &> 10\text{GeV}, \quad p_T^j > 20\text{GeV}, \quad E_T^{\text{miss}} > 10\text{GeV}, \\
\eta^\ell &< 2.5, \quad \eta^j < 5, \\
\Delta R_{jj} &> 0.4, \quad \Delta R_{\ell\ell} > 0.4
\end{aligned} \tag{28}$$

where p_T^ℓ and p_T^j are transverse momentum of leptons and jets respectively. E_T^{miss} is the missing transverse momentum. $\Delta R = \sqrt{\Delta\Phi^2 + \Delta\eta^2}$ is the separation in the rapidity-azimuth plane and η is the rapidity. The cuts are defined in the lab frame.

number of events	event selection	M_{recoil}	$p_T^{W(jj)}$	M_{trans}
n_S ($\sin\theta_H = 0.1$)	2.78	2.17	1.91	1.67
n_S ($\sin\theta_H = 0.2$)	12.03	9.35	8.24	7.21
n_S ($\sin\theta_H = 0.3$)	26.83	20.74	18.27	15.95
n_S ($\sin\theta_H = 0.4$)	47.30	36.38	32.01	27.82
$e^+e^- \rightarrow W^+W^-Z$	559.84	78.87	36.58	23.09
$e^+e^- \rightarrow ZZZ$	3.70	0.53	0.25	0.08
$e^+e^- \rightarrow W^+W^-W^+W^-$	1.71	0.16	0.10	0.01
$e^+e^- \rightarrow W^+W^-ZZ$	1.02	0.08	0.06	0
$e^+e^- \rightarrow ZZZZ$	0.006	0	0	0
n_B	566.28	79.64	36.98	23.18
$S(\sin\theta_H = 0.1)$	0.12	0.24	0.31	0.34
$S(\sin\theta_H = 0.2)$	0.50	1.03	1.31	1.43
$S(\sin\theta_H = 0.3)$	1.12	2.23	2.80	3.01
$S(\sin\theta_H = 0.4)$	1.96	3.81	4.69	4.98

TABLE I: The cut flow of the number of events for signal process A and backgrounds at the ILC. We have calculated for four typical values of $\sin\theta_H$. The values of discovery significance S at each step of cut are also shown.

The number of events (with luminosity=3000 fb⁻¹) of signal and backgrounds after event selection are listed in Table.I. We have calculated for four typical values of $\sin\theta_H$. n_S in the table is the number of signal events and n_B is the number of all background events. In order to improve the discovery significance, additional kinematic cuts are needed. We present distributions of signal and backgrounds as a function of various kinematic variables after event selection in Fig.3, including the recoil mass M_{recoil} of H_5^\pm , the transverse mass M_{trans} and the transverse momentum $p_T^{W(jj)}$ of the

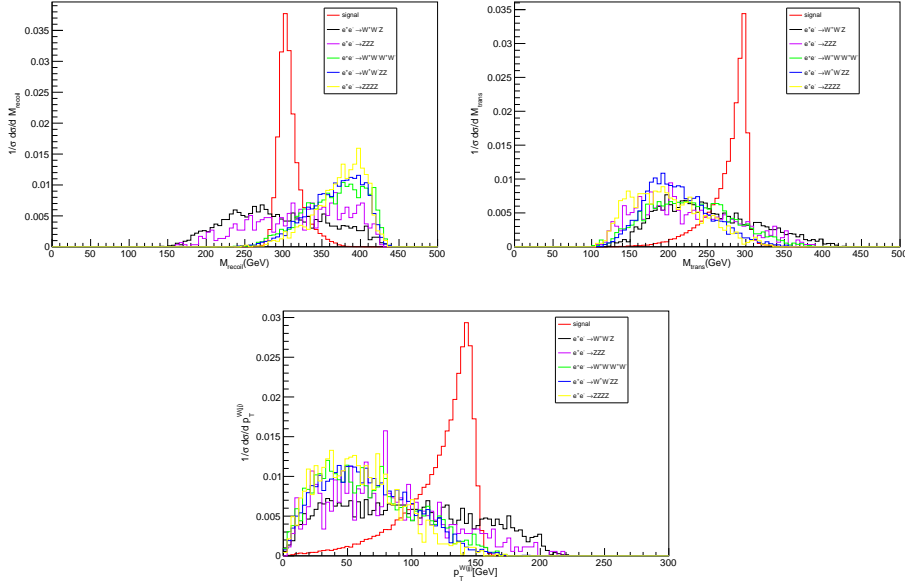


FIG. 3: The distributions of signal as well as backgrounds as a function of the recoil mass M_{recoil} , the transverse mass M_{trans} , and the transverse momentum $p_T^{W(jj)}$ of the reconstructed W after event selection in process A.

reconstructed W . From the distributions, we can see that the recoil mass M_{recoil} and the transverse mass M_{trans} of H_5^\pm for signal events form a peak around 300 GeV. The transverse momentum of the reconstructed W for signal events also has a peak. Therefore, in order to optimise the significance we use the following kinematic cuts:

$$\begin{aligned} 290 \text{ GeV} < M_{\text{recoil}} < 320 \text{ GeV}, \\ 95 \text{ GeV} < p_T^{W(jj)} < 152 \text{ GeV}. \end{aligned} \quad (29)$$

The above cuts are all related to jets system, no information from lepton system has been used. Turn to lepton system, we impose the following cut on the transverse mass constructed from leptons and missing transverse energy:

$$245 \text{ GeV} < M_{\text{trans}} < 305 \text{ GeV}. \quad (30)$$

The results of the number of events (with luminosity=3000 fb $^{-1}$) are shown in Table.I at each step of cut. The values of the discovery significance S are also shown. From the result in the table, we can find that the backgrounds mainly come from W^+W^-Z final states in SM. After all cuts the backgrounds can be reduced to several percentage of the one after event selection. For $\sin\theta_H=0.4$, the discovery significance is almost 5σ , so with more luminosity, the new scalar can be seen at the ILC.

B. Process B

In this scenario, the associated weak gauge boson decays leptonically, while the Z boson produced from the decay of H_5^\pm decays leptonically and W^\pm produced from H_5^\pm decays hadronically (process B). We adopt the same event selection criteria as in process A, i.e., three leptons, E_T^{miss} and more than or equal to 2 jets with $m_Z - 20 \text{ GeV} < M_{\text{inv}}^{Z(\ell\ell)} < m_Z + 20 \text{ GeV}$, $m_W - 20 \text{ GeV} < M_{\text{inv}}^{W(\text{jj})} < m_W + 20 \text{ GeV}$. We reconstruct H_5^\pm from the reconstructed W^\pm and Z bosons. The distributions

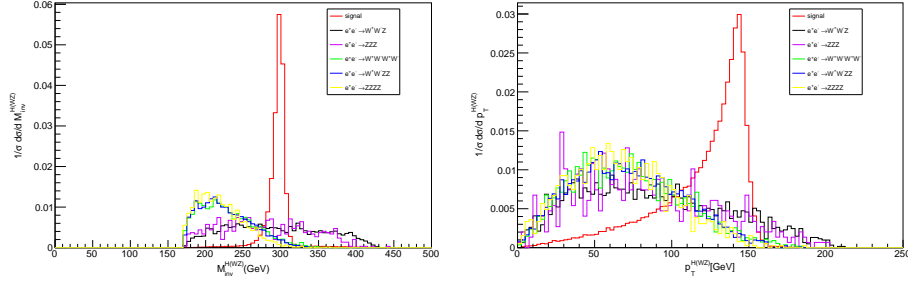


FIG. 4: The distributions of signal and backgrounds as a function of the $M_{\text{inv}}^{H(WZ)}$ and $p_T^{H(WZ)}$ after event selection in process B.

of signal and backgrounds as a function of the invariant mass $M_{\text{inv}}^{H(WZ)}$ of the reconstructed H_5^\pm , and the transverse momentum $p_T^{H(WZ)}$ of H_5^\pm after event selection are shown in Fig.4. According to the distributions, we impose the following Higgs mass window cut as well as the cut on $p_T^{H(WZ)}$ to improve the significance:

$$\begin{aligned} 290 \text{ GeV} < M_{\text{inv}}^{H(WZ)} < 310 \text{ GeV}, \\ 105 \text{ GeV} < p_T^{H(WZ)} < 175 \text{ GeV}. \end{aligned} \quad (31)$$

The results of the number of events (with luminosity=3000 fb⁻¹) are shown in Table.II at each step of cut. The values of discovery significance S are also shown. It is clear that after the cut on the reconstructed mass $M_{\text{inv}}^{H(WZ)}$ of H_5^\pm , the SM backgrounds reduced a lot. Further more, after all cuts the situation is better than that in process A. With two additional kinematic cuts less than 3 cuts in process A, the significance exceeds that in process A. The significance exceeds 5σ after all cuts for $\sin\theta_H = 0.4$. Therefore this channel could serve as a promising process searching for charged heavy Higgs particle.

number of events	event selection	$M_{\text{inv}}^{\text{H(WZ)}}$	$p_{\text{T}}^{\text{H(WZ)}}$
$n_{\text{S}} (\sin\theta_{\text{H}} = 0.1)$	2.93	2.22	1.75
$n_{\text{S}} (\sin\theta_{\text{H}} = 0.2)$	12.50	9.47	7.50
$n_{\text{S}} (\sin\theta_{\text{H}} = 0.3)$	28.37	21.42	16.94
$n_{\text{S}} (\sin\theta_{\text{H}} = 0.4)$	49.74	37.14	29.49
$e^+e^- \rightarrow W^+W^-Z$	559.84	49.15	21.03
$e^+e^- \rightarrow ZZZ$	3.70	0.26	0.07
$e^+e^- \rightarrow W^+W^-W^+W^-$	1.71	0.07	0.002
$e^+e^- \rightarrow W^+W^-ZZ$	1.02	0.04	0
$e^+e^- \rightarrow ZZZZ$	0.006	0	0
n_{B}	566.28	49.52	21.10
$S(\sin\theta_{\text{H}} = 0.1)$	0.12	0.31	0.38
$S(\sin\theta_{\text{H}} = 0.2)$	0.52	1.31	1.55
$S(\sin\theta_{\text{H}} = 0.3)$	1.18	2.86	3.31
$S(\sin\theta_{\text{H}} = 0.4)$	2.06	4.77	5.43

TABLE II: The cut flow of the number of events for signal process B and backgrounds at the ILC. We have calculated for four typical values of $\sin\theta_{\text{H}}$. The values of discovery significance S at each step of cut are also shown.

IV. SEARCHING FOR H_5^0

A. Process C

In the vector boson associated production processes another scalar can be produced, i.e., the neutral fiveplet H_5^0 . As mentioned above, a unique feature of the GM model is the mass degeneracy in each multiplet, therefore H_5^0 has the same mass with H_5^\pm and can be produced efficiently at 500 GeV at the ILC. In this section we study the production of neutral fiveplet in associated with a Z boson. H_5^0 decays to two W bosons subsequently. Notice the branching fractions of $H_5^0 \rightarrow ZZ$ and $H_5^0 \rightarrow W^+W^-$ are 64% and 36%, respectively. The relevant couplings are

$$g_{H_5^0 W^+W^-} = \sqrt{\frac{2}{3}} \frac{e^2 v_X}{s_w^2}, \quad g_{H_5^0 ZZ} = -\sqrt{\frac{8}{3}} \frac{e^2 v_X}{c_w^2 s_w^2}. \quad (32)$$

For the subsequent decay of W^+W^-Z , we consider two cases. In the first case we assume the associated weak gauge boson to decay hadronically, while the W^+W^- bosons produced from the decay of H_5^0 decay leptonically (process C), see Fig.5[left panel]. In this case, we can investigate

the possibility of measuring the recoil mass of H_5^0 by using the recoil method as in process A. The second decay mode we consider is that the associated weak gauge boson decays leptonically, while W^+W^- coming from H_5^0 decay hadronically(process D), see Fig.5[right panel]. In this case, we can reconstruct the H_5^0 from four jets. Moreover, we can calculate the recoil mass of H_5^0 using information of leptons.

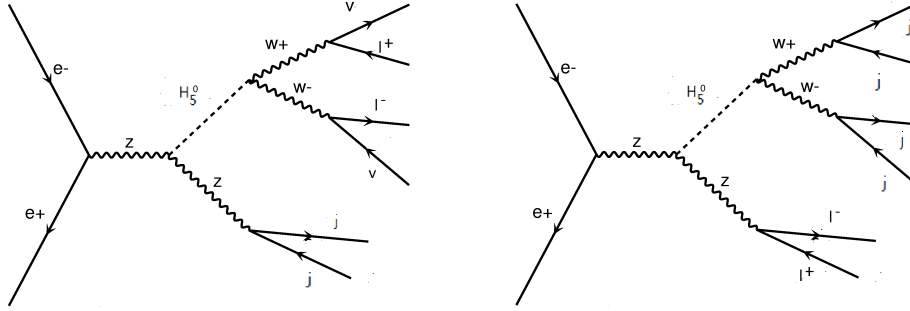


FIG. 5: The Feynman diagrams of the signal process C(left) and D(right) in the GM model.

For process C, in event selection we require the final states must contain two leptons, E_T^{miss} and more than or equal to 2 jets. We reconstruct Z boson by choosing two jets from final states such that their invariant mass is close to the Z boson mass most and further require that their invariant mass satisfy $m_Z - 20 \text{ GeV} < M_{\text{inv}}^{Z(jj)} < m_Z + 20 \text{ GeV}$. The selected events must satisfy the same basic cuts as in Eq.(28). The distributions of signal and backgrounds as a function of the recoil mass M_{recoil} calculated from jets information, the transverse momentum $p_T^{Z(jj)}$ of the reconstructed Z and the transverse mass M_{trans} after event selection are presented in Fig.6. From the plots, we use following kinematic cuts to improve the discovery significance:

$$\begin{aligned}
 292 \text{ GeV} &< M_{\text{recoil}} < 322 \text{ GeV}, \\
 95 \text{ GeV} &< p_T^{Z(jj)} < 145 \text{ GeV}, \\
 150 \text{ GeV} &< M_{\text{trans}} < 297 \text{ GeV}.
 \end{aligned} \tag{33}$$

The results of the number of events (with luminosity= 3000 fb^{-1}) at each step of the cut are shown in Table.III. The values of discovery significance S are also shown. The background events number in this case is very large after event selection. It is evident from the M_{trans} distribution that the signal and backgrounds have large overlap. So it is a difficult task to reduce the backgrounds effectively. The discovery potential of H_5^0 in this channel is bleak.

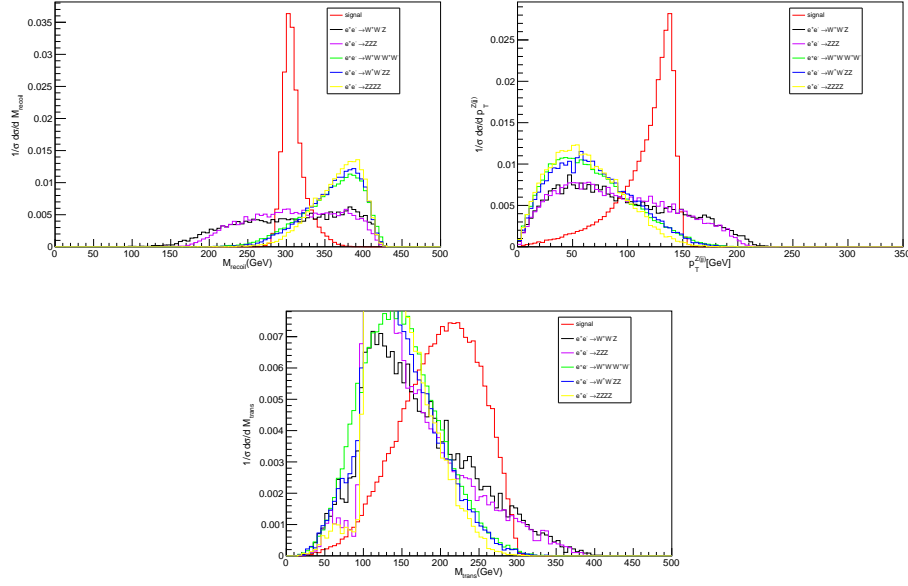


FIG. 6: The distributions of signal and backgrounds as a function of the recoil mass M_{recoil} , the transverse momentum $p_T^{Z(jj)}$ of Z and the transverse mass M_{trans} after event selection in process C.

B. Process D

The second decay mode we consider is that the associated weak gauge boson decays leptonically, while W^+W^- coming from H_5^0 decay hadronically, see right panel in Fig.5. For event selection we require the final states must contain two leptons, more than or equal to 4 jets. We reconstruct Z boson by requiring two lepton invariant mass satisfying $m_Z - 20 \text{ GeV} < M_{\text{inv}}^{Z(\ell\ell)} < m_Z + 20 \text{ GeV}$, since the leptons are from Z boson for signal. The selected events must satisfy the following similar basic cuts:

$$\begin{aligned}
 p_T^\ell &> 10 \text{ GeV}, \quad p_T^j > 20 \text{ GeV}, \\
 \eta^\ell &< 2.5, \quad \eta^j < 5, \\
 \Delta R_{jj} &> 0.4, \quad \Delta R_{\ell\ell} > 0.4.
 \end{aligned} \tag{34}$$

We can calculate the recoil mass of H_5^0 as in process A but with the information of leptons rather than jets. The recoiled mass of H_5^0 is given in terms of lepton energy $E^{\ell\ell}$ and lepton invariant mass $M_{\text{inv}}^{\ell\ell}$ as

$$M_{\text{recoil}}^2 = s - 2\sqrt{s}E^{\ell\ell} + M_{\text{inv}}^{\ell\ell 2} \tag{35}$$

where s is the center-of-mass energy in the collision. We reconstruct H_5^0 boson from jets system by choosing four jets from final states such that their invariant mass is close to the H_5^0 boson mass

number of events	event selection	M_{recoil}	$p_T^{Z(jj)}$	M_{trans}
$n_S (\sin\theta_H = 0.1)$	2.38	1.84	1.53	1.26
$n_S (\sin\theta_H = 0.2)$	9.58	7.44	6.18	5.07
$n_S (\sin\theta_H = 0.3)$	21.57	16.69	13.85	11.36
$n_S (\sin\theta_H = 0.4)$	38.07	29.21	24.14	19.81
$e^+e^- \rightarrow W^+W^-Z$	2060.14	260.38	139.90	86.18
$e^+e^- \rightarrow ZZZ$	72.02	11.84	6.30	3.71
$e^+e^- \rightarrow W^+W^-W^+W^-$	24.88	2.83	1.68	0.62
$e^+e^- \rightarrow W^+W^-ZZ$	3.62	0.37	0.27	0.08
$e^+e^- \rightarrow ZZZZ$	0.06	0.005	0.003	0
n_B	2160.73	275.42	148.16	90.60
$S(\sin\theta_H = 0.1)$	0.05	0.11	0.13	0.13
$S(\sin\theta_H = 0.2)$	0.21	0.45	0.50	0.53
$S(\sin\theta_H = 0.3)$	0.46	1.00	1.12	1.17
$S(\sin\theta_H = 0.4)$	0.82	1.73	1.93	2.01

TABLE III: The cut flow of the number of events for signal process C and backgrounds at the ILC. We have calculated for four typical values of $\sin\theta_H$. The values of discovery significance S at each step of cut are also shown.

most. The distributions of signal and backgrounds as a function of the reconstructed mass M_{inv}^{4j} of H_5^0 , the transverse momentum $p_T^{Z(\ell\ell)}$ of reconstructed Z boson and the recoil mass after event selection are presented in Fig.7. The recoil mass distribution in process D has a more sharp peak than that in process C. From these plots, in order to improve significance, the following cuts are imposed :

$$\begin{aligned}
250 \text{ GeV} &< M_{\text{inv}}^{4j} < 310 \text{ GeV}, \\
95 \text{ GeV} &< p_T^{Z(\ell\ell)} < 145 \text{ GeV}, \\
296 \text{ GeV} &< M_{\text{recoil}} < 306 \text{ GeV}.
\end{aligned} \tag{36}$$

The results of the cut flow of the number of events (with luminosity=3000 fb⁻¹) are shown in Table.IV. We find that the background events after event selection are much less than that in process C. After all cuts, the situation of process D is much better than that of process C.

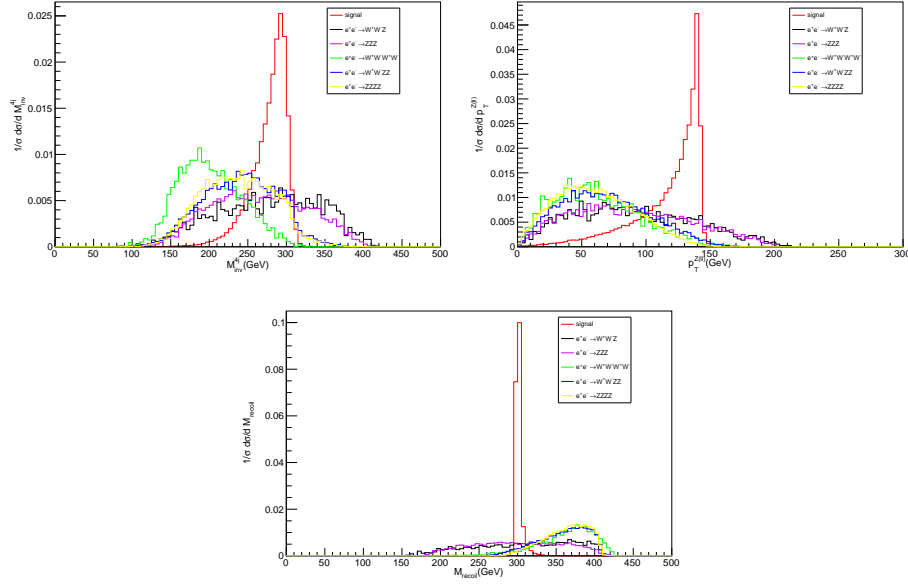


FIG. 7: The distributions of signal and backgrounds as a function of the M_{inv}^{4j} , $p_T^{Z(\ell\ell)}$ and M_{recoil} after event selection in process D.

V. MORE DISCUSSIONS ON PROCESS B

After the above comparison, we know that process B is the most “significant” channel, so it deserves a more detailed study. After all the cuts for signal process B and backgrounds imposed, we calculate the lowest necessary luminosity with 3σ and 5σ discovery significance as a function of $\sin\theta_H$ in Fig.8. It can be seen that high integrated luminosity is required to probe small $\sin\theta_H$. However, if no signal appears in the future collider, then the parameter triplet VEV v_X would be strictly constrained to be very small and the future experiment could compress the parameter space of the Georgi-Machacek model very sharply.

Having analysed the discovery potential for fixed fiveplet mass, now we turn our attention to another side, to discuss the discovery reach in the fiveplet mass for a fixed $\sin\theta_H$. We choose $\sqrt{s}=500$ GeV, $\sin\theta_H$ is taken to be 0.3, and let the fiveplet mass run in the range 200 GeV-450 GeV. In all cases the custodial triplet has a sufficiently large mass so that H_5^\pm has almost 100% branching ratio into $W^\pm Z$. The event selection criteria is the same as in process B. As discussed before, the cut on the invariant mass of the reconstructed H_5^\pm is useful to reduce backgrounds. Therefore we impose the invariant mass cut as following:

$$m_5 - 10 \text{ GeV} < M_{\text{inv}}^{H(WZ)} < m_5 + 10 \text{ GeV}, \quad (37)$$

For additional cut on the transverse momentum $p_T^{H(WZ)}$ of the reconstructed H_5^\pm , different cut

number of events	event selection	M_{inv}^{4j}	$p_T^{Z(\text{ll})}$	M_{recoil}
n_S ($\sin\theta_H = 0.1$)	2.01	1.75	1.42	1.31
n_S ($\sin\theta_H = 0.2$)	7.82	6.78	5.52	5.10
n_S ($\sin\theta_H = 0.3$)	18.07	15.69	12.74	11.67
n_S ($\sin\theta_H = 0.4$)	32.41	28.10	22.77	20.38
$e^+e^- \rightarrow W^+W^-Z$	566.93	173.74	79.10	16.23
$e^+e^- \rightarrow ZZZ$	42.33	13.57	5.44	0.99
$e^+e^- \rightarrow W^+W^-W^+W^-$	2.11	0.28	0.01	0
$e^+e^- \rightarrow W^+W^-ZZ$	1.81	0.69	0.08	0.004
$e^+e^- \rightarrow ZZZZ$	0.05	0.02	0.001	0
n_B	613.24	188.28	84.63	17.23
$S(\sin\theta_H = 0.1)$	0.08	0.13	0.15	0.31
$S(\sin\theta_H = 0.2)$	0.32	0.49	0.59	1.18
$S(\sin\theta_H = 0.3)$	0.73	1.13	1.35	2.56
$S(\sin\theta_H = 0.4)$	1.30	2.00	2.38	4.24

TABLE IV: The cut flow of the number of events for signal process D and backgrounds at the ILC. We have calculated for four typical values of $\sin\theta_H$. The values of discovery significance S at each step of cut are also shown.

should be applied for different fiveplet mass, as is evident from Fig.9. With increasing fiveplet mass, the position of the peak of $p_T^{H(WZ)}$ distribution goes downward to lower value of $p_T^{H(WZ)}$. Therefore, we perform a varying cut on $p_T^{H(WZ)}$, listed in Table.V. The signal and background events number at each stage of analysis at 500 GeV collision energy with 3000 fb^{-1} luminosity are listed in Table.V respectively for fiveplet mass $m_5 = 200, 250, 300, 350, 400 \text{ GeV}$. For $m_5 = 450 \text{ GeV}$, the cross section is very low and only the number of events after event selection is shown. We can see that for $m_5 \sim 200 \text{ GeV}$, the production rate is relatively high at 500 GeV collision energy and the significance exceeds 5σ . But for larger $m_5 (> 400 \text{ GeV})$, the situation is worse due to small collision energy compared with fiveplet mass. For such a heavy particle, 1 TeV collision energy is more suited.

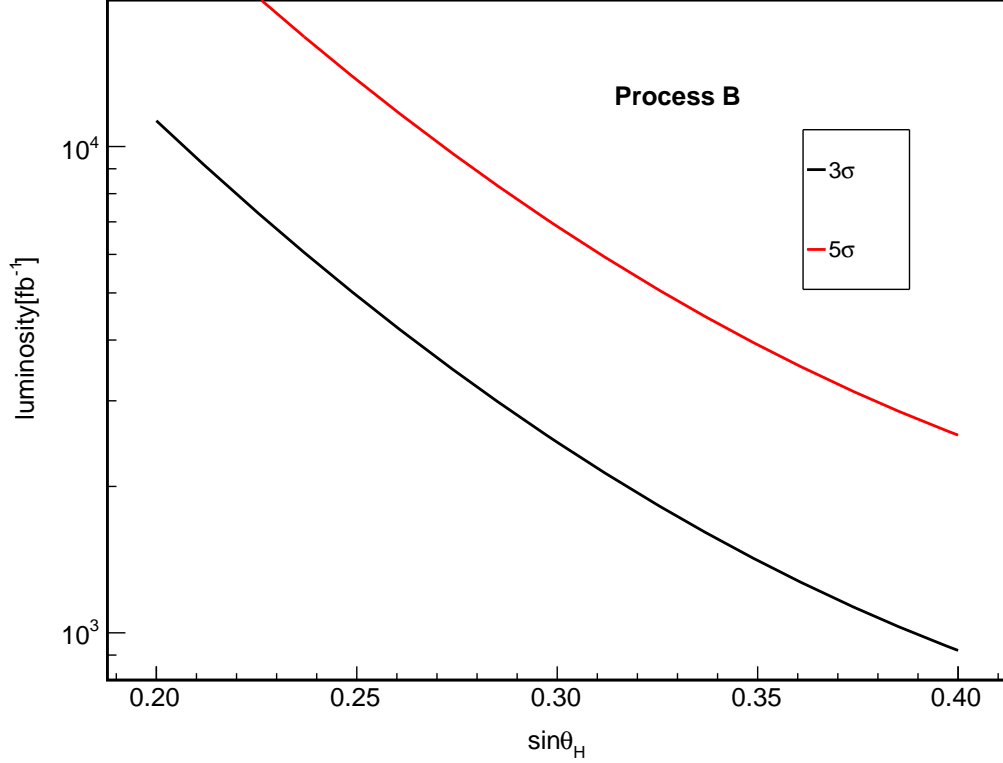


FIG. 8: The lowest necessary luminosity with 3σ and 5σ discovery significance for process B at collision energy 0.5 TeV at the ILC.

VI. TESTING THE MASS DEGENERACY OF CHARGED AND NEUTRAL SCALARS

In the analysis of process D, we have not considered the decay process $H^0 \rightarrow ZZ$, which contributes to our signal when two Z bosons decay to jets and one Z decays to leptons. Moreover, a distinguished feature of GM model is the mass degeneracy within each multiplet. Therefore a simultaneously observation of the distinctive peaks at the same position in the invariant mass distributions of $M_{\text{inv}}^{\text{WW}}$ and $M_{\text{inv}}^{\text{WZ}}$ is a signature of the GM model[11]. In order to achieve this goal it is important to distinguish WW and ZZ in the final states. In process B and process D discussed above, we have chosen the mass window cut on the invariant mass of reconstructed W or Z to be $\pm 20\text{GeV}$. In order to test the mass degeneracy of charged and neutral scalar bosons, a more strict invariant mass cut is necessary. So in process B, with the other kinematic cuts unchanged, we further require the mass window cut on the invariant mass of the reconstructed W and Z to be $\pm 10\text{GeV}$. In process D, we keep the other additional kinematic cuts unchanged and replace the cut on M_{inv}^{4j} with the following condition: two W bosons must be reconstructed from four of all jets in final states such that the invariant mass of both reconstructed W bosons satisfy

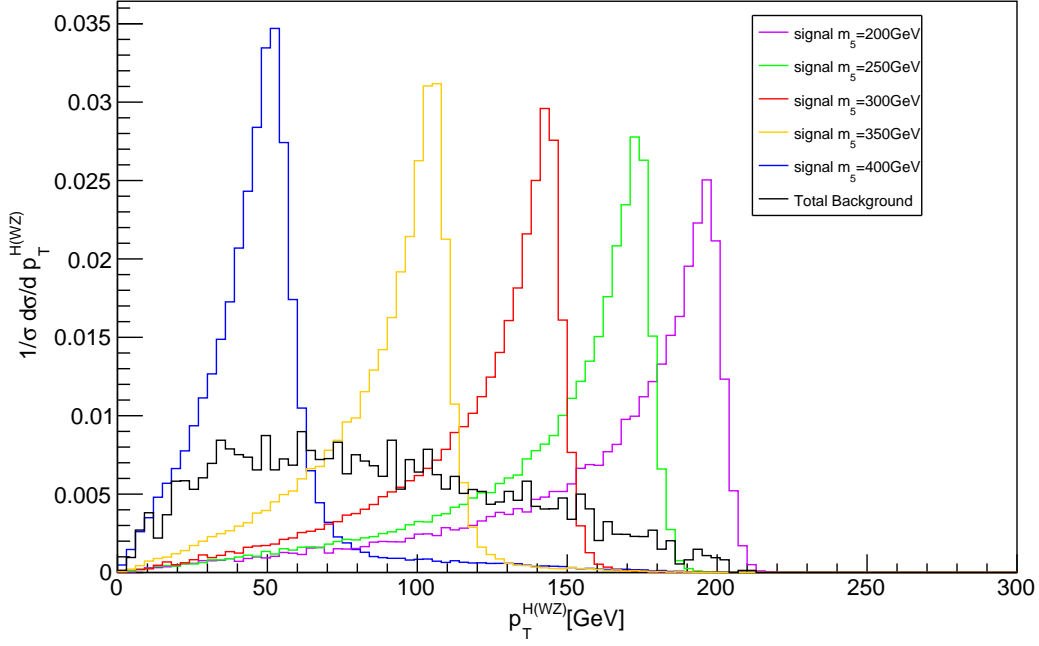


FIG. 9: The transverse momentum $p_T^{H(WZ)}$ distributions of the reconstructed H_5^\pm for fiveplet mass $m_5 = 200, 250, 300, 350, 400$ GeV in process B as well as total backgrounds after event selection at collision energy 0.5 TeV at the ILC.

$m_W - 10 \text{ GeV} < M_{\text{inv}}^{W(jj)} < m_W + 10 \text{ GeV}$, and the invariant mass of the reconstructed H_5^0 from two W bosons satisfy the same cut as for M_{inv}^{4j} . The results are listed in Table.VI for $\mathcal{L} = 3000 \text{ fb}^{-1}$ and 5000 fb^{-1} respectively. The results in Table.VI show that the significance would decline if more strict invariant mass window cut on the reconstructed W or Z bosons are imposed. This is not surprising since the final state radiation would carry away some amount of energy and momentum. Nevertheless, with high luminosity 5000 fb^{-1} , more than 3σ discovery significance can be reached for neutral fiveplet scalar when $\sin\theta_H = 0.4$, while larger than 5σ discovery significance is obtained for charged fiveplet scalar.

VII. CONCLUSIONS

The existence of exotic particles in new physics beyond the Standard Model is highly expected among the particle physicists community. The Georgi-Machacek model is one of many Beyond Standard Model scenarios with an extended scalar sector which can group under the custodial $SU(2)_C$ symmetry into a fiveplet, a triplet, and two singlets. In this paper, we have studied

process B		n_S	n_B	S
$m_5 = 200$ GeV	Event Selection	31.77	566.28	1.32
	$M_{\text{inv}}^{\text{H(WZ)}} \in [190, 210]$ GeV	28.04	43.19	3.90
	$p_T^{\text{H(WZ)}} \in [145, 220]$ GeV	22.06	12.44	5.12
$m_5 = 250$ GeV	Event Selection	38.62	566.28	1.60
	$M_{\text{inv}}^{\text{H(WZ)}} \in [240, 260]$ GeV	31.61	61.28	3.75
	$p_T^{\text{H(WZ)}} \in [120, 190]$ GeV	26.56	25.09	4.63
$m_5 = 300$ GeV	Event Selection	28.37	566.28	1.18
	$M_{\text{inv}}^{\text{H(WZ)}} \in [290, 310]$ GeV	21.42	49.52	2.86
	$p_T^{\text{H(WZ)}} \in [105, 175]$ GeV	16.94	21.10	3.31
$m_5 = 350$ GeV	Event Selection	16.13	566.28	0.67
	$M_{\text{inv}}^{\text{H(WZ)}} \in [340, 360]$ GeV	11.50	44.15	1.66
	$p_T^{\text{H(WZ)}} \in [80, 115]$ GeV	8.26	17.89	1.83
$m_5 = 400$ GeV	Event Selection	5.66	566.28	0.24
	$M_{\text{inv}}^{\text{H(WZ)}} \in [390, 410]$ GeV	3.80	30.68	0.67
	$p_T^{\text{H(WZ)}} \in [35, 60]$ GeV	2.71	13.06	0.73
$m_5 = 450$ GeV	Event Selection	0.0018	566.28	7.5×10^{-5}

TABLE V: Number of events for GM process B signal n_S and SM backgrounds n_B after event selection, fiveplet scalar mass window cut $M_{\text{inv}}^{\text{H(WZ)}} \in [m_5 - 10, m_5 + 10]$ GeV and a further sliding cut on $p_T^{\text{H(WZ)}}$ at 500 GeV ILC (for $\mathcal{L} = 3000 \text{ fb}^{-1}$), respectively for fiveplet mass $m_5 = 200, 250, 300, 350, 400$ GeV. For $m_5 = 450$ GeV, the cross section is very low and only the number of events after event selection is shown. The parameter $\sin\theta_H$ is taken to be 0.3. The values of discovery significance S at each step of cut are also shown.

the collider phenomenology of the heavy charged and neutral fiveplet Higgs (H_5^\pm and H_5^0) at the International Linear Collider(ILC). We focus on the vector boson associated production process, and discuss two decay modes for both charged and neutral fiveplet scalars. In process A the associated weak gauge boson is assumed to decay hadronically, while the $W^\pm Z$ bosons produced from the decay of H_5^\pm decay leptonically. In this case, we can measure the recoil mass of H_5^\pm by using the recoil method at the ILC, and construct the transverse mass for the $3\ell + E_T^{\text{miss}}$ system. In process B the associated weak gauge boson is assumed to decay leptonically, while the W^\pm produced from H_5^\pm decays hadronically and the Z boson produced from H_5^\pm decays leptonically. We find that process B is better than process A for discovering the charged fiveplet. We also considered the search

number of events	B(3000 fb ⁻¹)	B(5000 fb ⁻¹)	D(3000 fb ⁻¹)	D(5000 fb ⁻¹)
n _S (sinθ _H = 0.1)	1.48	2.47	0.57	0.94
n _S (sinθ _H = 0.2)	6.35	10.58	2.19	3.64
n _S (sinθ _H = 0.3)	14.36	23.94	5.01	8.35
n _S (sinθ _H = 0.4)	24.86	41.43	8.77	14.61
n _B	17.89	29.82	8.55	14.26
S(sinθ _H = 0.1)	0.35	0.45	0.19	0.25
S(sinθ _H = 0.2)	1.42	1.84	0.72	0.93
S(sinθ _H = 0.3)	3.05	3.93	1.58	2.04
S(sinθ _H = 0.4)	4.98	6.42	2.63	3.39

TABLE VI: The number of events with more strict cuts on the invariant mass of reconstructed W or Z bosons for process B, D and total backgrounds. We have calculated for four typical values of sinθ_H and two values of luminosity ($\mathcal{L} = 3000 \text{ fb}^{-1}$ and 5000 fb^{-1}). The values of discovery significance S are also shown.

strategy for the neutral fiveplet. Again we compared two decay processes. In the first case we assume the associated weak gauge boson to decay hadronically, while the W^+W^- bosons produced from the decay of H_5^0 decay leptonically (process C). The second decay mode we consider is that the associated weak gauge boson decays leptonically, while W^+W^- coming from H_5^0 decay hadronically (process D). We find that process D is better than process C for discovering the neutral fiveplet. We find that in all four processes, process B is most promising to serve as the discovery process after several cuts. The charged scalar can be seen at the ILC in this channel with the discovery significance exceeds 5σ for relatively large sinθ_H. The lowest necessary luminosity with 3σ and 5σ discovery significance are calculated as a function of the triplet VEV v_X for process B. The future high luminosity collider experiment could measure the value of the triplet VEV v_X in the GM model or otherwise put a stringent constraint on it. The discovery reach in the fiveplet mass for a fixed sinθ_H are discussed, the situation is better for relatively light scalar than heavy scalar. Lastly, testing the mass degeneracy of charged and neutral scalar bosons as a direct evidence of GM model has been analysed. It is possible to check this property at 5000 fb^{-1} ILC with over 3σ significance for relatively large sinθ_H.

Acknowledgments

This work is supported by the National Natural Science Foundation of China (Grant No. 11675033, 11675034), by the Fundamental Research Funds for the Central Universities (Grant No. DUT15LK22).

-
- [1] G. Aad, et al., [ATLAS Collaboration], *Observation of a new particle in the search for the Standard Model Higgs boson with the ATLAS detector at the LHC*, Phys. Lett. B 716, 1-29 (2012), [arXiv:1207.7214].
 - [2] S. Chatrchyan, et al., [CMS Collaboration], *Observation of a new boson at a mass of 125 GeV with the CMS experiment at the LHC*, Phys. Lett. B 716, 30 (2012), [arXiv:1207.7235].
 - [3] T.D.Lee, *A Theory of Spontaneous T Violation*, Phys. Rev. D 8, 1226(1973) . G.C.Branco, P.M.Ferreira, L.Lavoura, M.N.Rebelo, Marc Sher, Joao P.Silva, *Theory and phenomenology of two-Higgs-doublet models*, Phys. Rept. 516 , 1(2012), [arXiv:1106.0034].
 - [4] H.P. Nilles, *Supersymmetry, Supergravity and Particle Physics*, Phys. Rept.110, 1 (1984); H.E. Haber and G.L. Kane, *The search for supersymmetry: probing physics beyond the standard model*, Phys. Rept.117, 75 (1985); R. Barbieri, *Looking beyond the standard model: the supersymmetric option*, Riv. Nuovo Cim.11N4,1 (1988).
 - [5] R. N. Mohapatra and J. C. Pati, *A Natural Left Right Symmetry*, Phys. Rev. D 11, 2558 (1975); G. Senjanovic and R. N. Mohapatra, *Exact Left Right Symmetry and Spontaneous Violation of Parity*, Phys. Rev. D 12, 1502 (1975).
 - [6] N. Arkani-Hamed, A. G. Cohen, E. Katz and A. E. Nelson, *The lightest Higgs 2002*, JHEP 0207, 034 (2002);
 - [7] H. Georgi and M. Machacek, *Doubly Charged Higgs Bosons*, Nucl. Phys. B262, 463 (1985).
 - [8] J. F. Gunion, R. Vega and J. Wudka, *Higgs triplets in the standard model*, Phys. Rev. D42,1673(1990).
 - [9] M. S. Chanowitz and M. Golden, *Higgs Boson Triplets With $M_W = M_Z \cos \theta_W$* , Phys. Lett. B 165, 105 (1985).
 - [10] T. P. Cheng and L. F. Li, *Neutrino masses, mixings and oscillations in $SU(2) \times U(1)$ models of electroweak interactions*, Phys. Rev. D 22, 2860 (1980); J. Schechter and J. W. F. Valle, *Neutrino masses in $SU(2) \times U(1)$ theories*, Phys. Rev. D 22, 2227(1980); G. Lazarides, Q. Shafi and C. Wetterich, *Proton lifetime and fermion masses in an $SO(10)$ model*, Nucl. Phys. B 181, 287 (1981); R. N. Mohapatra and G. Senjanovic, *Neutrino masses and mixings in gauge models with spontaneous parity violation*, Phys. Rev. D 23,165 (1981) ; M. Magg and C. Wetterich, *Neutrino mass problem and gauge hierarchy*, Phys. Lett. B 94, 61 (1980).

- [11] C.W.Chiang, S.Kanemura and K.Yagyu, *Phenomenology of the Georgi-Machacek model at future electron-positron colliders*, Phys. Rev. D 93, 055002 (2016), [arXiv:1510.06297].
- [12] C.W.Chiang, A.L.Kuo and T.Yamada, *Searches of exotic Higgs bosons in general mass spectra of the Georgi-Machacek model at the LHC*, JHEP1601,120(2016), [arXiv:1511.00865]. C.W.Chiang and K.Tsumura, *Properties and searches of the exotic neutral Higgs bosons in the Georgi-Machacek model*, JHEP1504,113(2015), [arXiv:1501.04257].
- [13] C.W.Chiang and K.Yagyu, *Testing the custodial symmetry in the Higgs sector of the Georgi-Machacek model*, JHEP1301,026(2013), [arXiv:1211.2658].
- [14] Stephen Godfrey and Ken Moats, *Exploring Higgs Triplet Models via Vector Boson Scattering at the LHC*, Phys.Rev.D81,075026(2010), [arXiv:1003.3033].
- [15] C.Degrande, K.Hartling, H.E.Logan, A.D.Peterson and M.Zaro, *Automatic predictions in the Georgi-Machacek model at next-to-leading order accuracy*, Phys. Rev. D 93, 035004 (2016), [arXiv:1512.01243].
- [16] C.Englert, E.Re and M.Spannowsky, *Pinning down Higgs triplets at the LHC*, Phys. Rev. D88,(2013) 035024, [arXiv:1306.6228].
- [17] Spencer Chang, Christopher A. Newby, Nirmal Raj, Chaowaroj Wanotayaroj, *Revisiting Theories with Enhanced Higgs Couplings to Weak Gauge Bosons*, Phys. Rev. D86, 095015(2012), [arXiv:1207.0493].
- [18] Cheng-Wei Chiang, An-Li Kuo, Kei Yagyu, *Enhancements of weak gauge boson scattering processes at the CERN LHC*, JHEP 1310,072(2013), [arXiv:1307.7526].
- [19] H. E. Logan and M. A. Roy, *Higgs couplings in a model with triplets*, Phys. Rev. D 82, 115011 (2010), [arXiv:1008.4869].
- [20] A. Falkowski, S. Rychkov and A. Urbano, *What if the Higgs couplings to W and Z bosons are larger than in the Standard Model?* JHEP 1204, 073 (2012), [arXiv:1202.1532].
- [21] J. A. Grifols and A. Mendez, *$W^\mp Z H^\pm$ coupling in $SU(2) \times U(1)$ gauge models*, Phys. Rev. D 22, 1725 (1980); M. C. Peyranere, H. E. Haber and P. Irulegui, *$H^\pm \rightarrow W^\pm \gamma$ and $H^\pm \rightarrow W^\pm Z$ in two-Higgs-doublet models: Large-fermion-mass limit*, Phys. Rev. D 44, 191 (1991); J. L. Diaz-Cruz, J. Hernandez-Sanchez and J. J. Toscano, *An effective Lagrangian description of charged Higgs decays $H^+ \rightarrow W^+ \gamma$, $W^+ Z$ and $W^+ h^0$* , Phys. Lett. B512, 339 (2001); E. Asakawa and S. Kanemura, *The $H^\pm W^\pm Z^0$ vertex and single charged Higgs boson production via WZ fusion at the large hadron collider*, Phys. Lett. B 626,111 (2005), [arXiv:0506310]; E. Asakawa, S. Kanemura and J. Kanzaki, *Potential for measuring the $H^\pm W^\pm Z^0$ vertex from WZ fusion at the Large Hadron Collider*, Phys. Rev. D 75, 075022 (2007), [arXiv:0612271].
- [22] S. Kanemura, K. Yagyu and K. Yanase, *Testing Higgs models via the $H^\pm W^\mp Z$ vertex by a recoil method at the International Linear Collider*, Phys. Rev. D 83, 075018 (2011).
- [23] K. Hartling, K. Kumar and H. E. Logan, *The decoupling limit in the Georgi-Machacek model*, Phys. Rev. D90,015007(2014), [arXiv:1404.2640].
- [24] The ATLAS and CMS Collaborations, *Measurements of the Higgs boson production and decay rates and constraints on its couplings from a combined ATLAS and CMS analysis of the LHC pp collision*

- data at $\sqrt{s} = 7$ and 8 TeV, ATLAS-CONF-2015-044.
- [25] K. Hartling, K. Kumar and H. E. Logan, *Indirect constraints on the Georgi-Machacek model and implications for Higgs couplings*, Phys. Rev. D91,015013(2015), [arXiv:1410.5538].
 - [26] M. E. Peskin and T. Takeuchi, *Estimation of oblique electroweak corrections*, Phys.Rev.D46,381(1992).
 - [27] The ATLAS Collaboration, *Search for a Charged Higgs Boson Produced in the Vector-boson Fusion Mode with Decay $H^\pm \rightarrow W^\pm Z$ using pp Collisions at $\sqrt{s} = 8$ TeV with the ATLAS Experiment*, Phys. Rev. Lett. 114, 231801 (2015), [arXiv:1503.04233].
 - [28] C. W. Chiang, S. Kanemura and K. Yagyu, *Novel Constraint on Parameter Space of the Georgi-Machacek Model by Current LHC Data*, Phys. Rev. D 90 115025 (2014), [arXiv:1407.5053].
 - [29] H.E.Logan and M.Zaro, *Recommendations for the interpretation of LHC searches for H_5^0, H_5^\pm , and $H_5^{\pm\pm}$ in vector boson fusion with decays to vector boson pairs*, <https://cds.cern.ch/record/2002500>.
 - [30] K.Hartling, K.Kumar and H.E.Logan, *GMCALC: a calculator for the Georgi-Machacek model*, [arXiv:1412.7387].
 - [31] A. Alloul, N. D. Christensen, C. Degrande, C. Duhr, and B.Fuks, *FeynRules 2.0 - A complete toolbox for tree-level phenomenology*, Comput. Phys. Commun. 185, 2250-2300 (2014), [arXiv:1310.1921].
 - [32] C. Degrande, C. Duhr, B. Fuks, D. Grellscheid, O.Mattelaer, and T. Reiter, *UFO the universal Feyn-Rules output*, Comput. Phys. Commun. 183, 1201-1214 (2012), [arXiv:1108.2040].
 - [33] J. Alwall, R. Frederix, S. Frixione, V. Hirschi, F. Maltoni, O. Mattelaer, H.-S. Shao, T. Stelzer, P. Torrielli, and M. Zaro, *The automated computation of tree-level and next-to-leading order differential cross sections, and their matching to parton shower simulations*, JHEP 1407, 079 (2014), [arXiv:1405.0301].
 - [34] T. Sjostrand, S. Mrenna, P.Z. Skands, *PYTHIA 6.4 Physics and Manual*, JHEP 0605, 026 (2006).
 - [35] J.de Favereau, et al, DELPHES 3 Collaboration, *DELPHES 3, A modular framework for fast simulation of a generic collider experiment*, JHEP 1402,057(2014).
 - [36] M.Cacciari, G.P.Salam, G.Soyez, *The anti- k_t jet clustering algorithm*, JHEP 0804,063(2008).